

Cross sections for  $K$ - and  $L$ -shell excitation in slow-ion—atom collisions

D. Schneider and N. Stolterfoht

*Hahn-Meitner-Institut für Kernforschung GmbH, Bereich Kern- und Strahlenphysik,  
Glienicke Strasse 100, 1000 Berlin 39, West Germany*

(Received 12 November 1980)

Absolute cross sections for Auger-electron production were measured for the target atom Ar bombarded by  $B^+$ ,  $C^+$ ,  $N^+$ ,  $O^+$ , and  $Ne^+$  ions at energies from 50 to 600 keV. Cross sections for  $L$ -shell excitation of the target atom and the  $K$ -shell excitation of the projectiles were deduced. The sum of the  $L$ - and  $K$ -shell excitation cross sections are found to increase monotonically with decreasing nuclear charge of the projectiles. The data are interpreted in terms of adiabatic molecular orbital (MO) diagrams. Evidence is found for electron promotion via the  $3d\sigma$  MO being the dominant mechanism which is responsible for the inner-shell vacancy production.

## I. INTRODUCTION

Many experimental results on heavy-ion—atom collisions have proven that the molecular orbital (MO) model<sup>1,2</sup> provides a useful framework for the understanding of the production of inner-shell vacancies, if the velocity of the projectile ions is smaller than those of the relevant inner-shell electrons. Within the MO model various theoretical approaches have been developed to describe different modes of coupling<sup>3–5</sup> between MO's. For  $K$ -vacancy-production cross sections, in general, good agreement between experimental results and theoretical predictions have been shown for a large variety of symmetric and near-symmetric collision systems.<sup>6–8</sup>

Vacancy production in the  $L$  shell has also been the subject of considerable work.<sup>9–13</sup> For the well-studied symmetric Ar+Ar system unexpectedly high cross sections for the vacancy production in the  $L$  shell were found experimentally.<sup>10</sup> The high probability for the  $L$ -shell excitation is inferred from the diabatic  $4f\sigma$  MO which is formed during the collision and which crosses various unfilled orbitals. Owing to these crossings, the probability for a transfer of the  $L$ -shell electrons into higher vacant levels is large. When the ion-atom system separates, the electron remains in these higher-lying levels. Within this picture simple models have been proposed by Kessel and co-workers<sup>10,11</sup> and by Fortner *et al.*<sup>12</sup> in order to interpret the vacancy-production cross sections. In the model used by Kessel and co-workers<sup>10,11</sup> a step-functional form for the probability of the  $L$ -shell

excitation of Ar versus the impact parameter is assumed. This was justified by experimental results from measurements of the projectile energy loss and measurements<sup>9,11</sup> of Auger-electron emission.<sup>10</sup> The empirically deduced critical distance for the production of inner-shell vacancies shows good agreement with the theoretically predicted abrupt rise of the  $4f\sigma$  orbital.

Apart from the studies on near-symmetric systems the vacancy production in  $L$  and  $K$  shells in asymmetric collision systems was investigated.<sup>8,13–17</sup> In these studies primarily heavy systems have been investigated; low- $Z$  systems have been studied comparably little so far. It was found that the sum of  $L$ - and  $K$ -vacancy production in the higher- and the lower- $Z$  collision partner, respectively, under conditions of  $K$ - $L$  level matching, yields the vacancy-formation probability in the  $3d\sigma$  molecular orbital.

In this work absolute vacancy-production cross sections for the  $L$  shell of the target atom Ar and for the  $K$  shell in projectile ions with  $Z$  ranging from 5 to 10 are deduced from Auger-electron measurements. From these data the sum of the cross sections and cross-section ratios can be deduced. Since the total cross sections and cross-section ratios refer to different coupling mechanisms in the MO model, we present these data in two different communications.

Cross-section ratios have been published previously,<sup>8,15,18</sup> where a detailed theoretical analysis was performed.<sup>8,18</sup> Therefore the cross-section ratio will not be investigated here. In the present work the summed cross sections for the total inner-shell

vacancy production will be discussed. To interpret the results, adiabatic MO correlation diagrams are calculated and compared to the experimental data. It will be shown by means of MO correlation diagrams that inner-shell excitation is probably caused by electron promotion via the  $3d\sigma$  orbital.

In Sec. II the experimental procedure for the determination of the cross sections is described and the experimental results are presented. In Sec. III the cross sections are discussed in terms of adiabatic MO diagrams.

## II. EXPERIMENTAL RESULTS

The experimental apparatus has been described in detail previously in Refs. 6 and 18 (and references therein), so that it will be mentioned only briefly here. The experiments were performed in a crossed-beam apparatus. The ion beams were produced by an AN Van de Graaff accelerator and were crossed with a gas target beam in the scattering chamber. The secondary electrons emitted from the scattering volume were analyzed with a parallel-plate electrostatic electron analyzer. The electron observation angle could be varied from  $15^\circ$  to  $160^\circ$  relative to the beam axis, so that the angular distribution of Auger electrons could be determined. Thus, by choosing an appropriate observation angle, the Auger peak of the target could be separated from that of the kinematically (Doppler) shifted peak of the projectile. The spectroscopic resolution of the spectrometer was 5.2% full width at half maximum; this relatively low resolution and correspondingly higher transmission was chosen because of low cross sections present in some cases. Since the spectrometer efficiency and the gas target pressure were determined from auxiliary measurements,<sup>6,19</sup> absolute cross sections for Auger-electron production could be deduced.

Typical electron emission spectra are shown in Figs. 1(a)–1(c). The curves show broad peak structures which are superimposed upon a continuous distribution of electron background. The structures are attributed to Auger transitions stemming either from projectile or target excitation, respectively. Peaks due to *K*-shell Auger electrons from the projectiles and due to *L*-shell Auger electrons from the Ar target are clearly identified in the spectra.

Since electrons were analyzed at energies well above and below the Auger structures, a background function could be determined by fitting the logarithm of the continuum cross section which

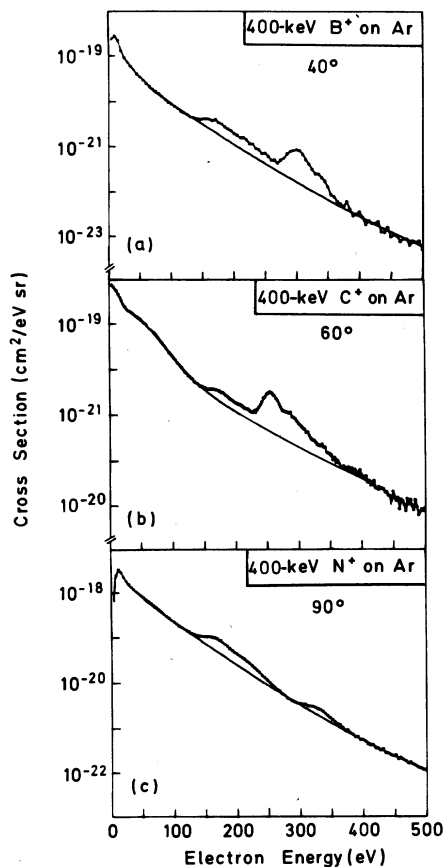


FIG. 1. Double differential cross sections for electron production from 400-keV  $B^+$ ,  $C^+$ , and  $N^+$  on Ar collisions. The spectra are taken at different observation angles. The analytical background function is indicated as a solid line. A broad peak structure at about 100 eV is discussed in detail in Ref. 20.

could then be subtracted. Background-subtracted spectra are shown in Figs. 2a–2(c), where the energetically well separated peaks are indicated due to *K*- and *L*-shell Auger electrons from the projectile and the target, respectively. It should be pointed out that the determination of the actual shape of the background function is somewhat uncertain. This is partly due to an additional broad structure near 100 eV which is close to the observed projectile and target Auger lines. It is found that this structure varies in intensity as the observation angle is changed. Its position in electron energy, however, remains unchanged. The origin for this structure is not clear at present, but it seems specifically to be related to the Ar target atom. More details concerning this structure are given in Ref. 20.

Total cross sections for Auger-electron produc-

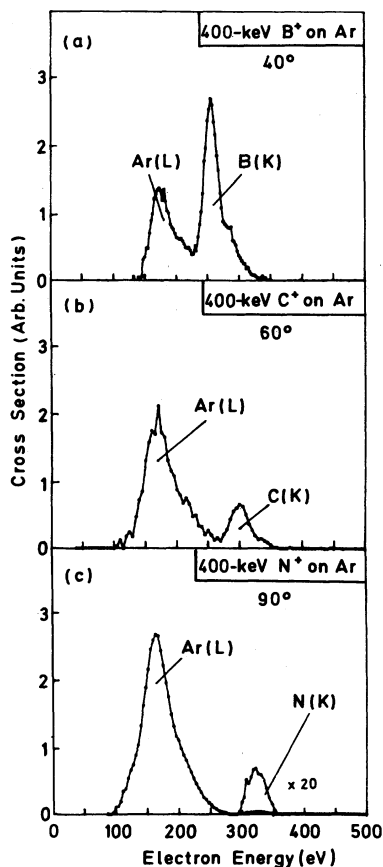


FIG. 2. Double differential cross section for Auger-electron production after subtraction of the continuous electron background. The structure due to the  $L$ -shell excitation in Ar and due to the  $K$ -shell excitation in the different projectile ions is indicated.

tion were deduced by numerical integration over angle and energy of the corresponding Auger-electron spectra. The cross sections for Auger-electron production in the projectile atoms were corrected for anisotropy caused by the collision kinematics. Details concerning this correction are given in Ref. 19. The data showed that the Auger-electron emission can be assumed to be isotropic within the accuracy of these measurements. Therefore, in general, cross sections were obtained from spectra taken at one angle. Some of the cross sections are mean values with respect to different observation angles. In Table I the absolute Auger-electron production cross sections are given for the  $K$  Auger electrons from the projectiles  $\sigma_P(K)$  and for the  $L$  Auger-electron production in the Ar target  $\sigma_T(L)$ .

The cross sections for  $K$  and  $L$  Auger-electron production are set to be equal to the corresponding  $K$ - and  $L$ -shell vacancy-production cross sections. In doing so radiative transitions were neglected. It should be noted that especially for the Ar- $L$  fluorescence yield, strong variations with the degree of outer-shell ionization have been reported.<sup>21</sup> However, despite this, the mean fluorescence yield is expected to be much smaller than one. Therefore, variation of the Auger yield is expected to be small. For the investigated collision systems it is assumed that fluorescence-yield effects would not cause more than 10% uncertainty.

Auger-electron production via higher-order effects produce electrons outside the integration area. Other contributions of Auger electrons which may

TABLE I. Absolute cross sections for  $K$ - and  $L$ -shell ionization for various projectile ions and the target atom Ar.

Projectile energy (keV)	System cross section ( $10^{-20}$ cm <sup>2</sup> )									
	$B^+ + Ar$		$C^+ + Ar$		$N^+ + Ar$		$O^+ + Ar$		$Ne^+ + Ar$	
	$\sigma_B$	$\sigma_{Ar}$	$\sigma_C$	$\sigma_{Ar}$	$\sigma_N$	$\sigma_{Ar}$	$\sigma_O$	$\sigma_{Ar}$	$\sigma_{Ar}$	$\sigma_{Ar}$
35					0.155	412				
40					0.18	443				
50					0.29	460			444	116
70	493	134	32.2	441	0.39	495	0.032	492		130
100	578	215	60.6	577	1.19	613	0.056	528		184
150							0.078	580		
200	745	440	135	903	4.85	704	0.128			
300	741	571							781	
400	814	667	240	1079	17.9	802	1.19	954		400
600	920	818	355	1170	37.7	884				

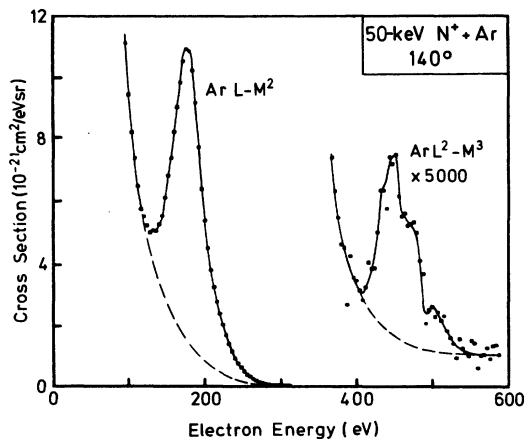


FIG. 3. Double differential cross sections for electron production in 50-keV  $N^+$  on Ar collisions. Observation angle is  $140^\circ$ . The peaks are due to Ar  $L-M^2$  and Ar  $L^2-M^3$  transitions (Ref. 20).

result from a multiply ionized  $L$  shell and which would fall outside the integration area are assumed to be small. As an example this is shown in Fig. 3 where Auger-electrons due to double ionization of the  $L$  shell followed by a correlated two-electron transition have been observed in 50-keV  $N^+$  on Ar collisions.<sup>20</sup> Their contribution is less than 0.001.

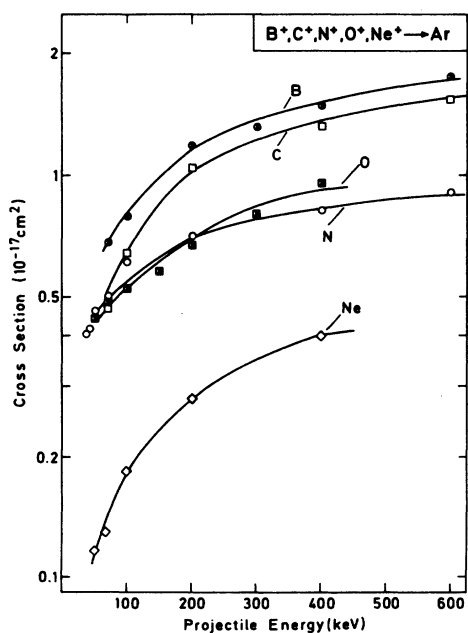


FIG. 4. Summed  $K$ - and  $L$ -shell vacancy production cross sections as obtained from the target [ $\sigma_T(L)$ ] and the projectile [ $\sigma_P(K)$ ] Auger-electron emission versus impact energy.

The uncertainty for the absolute cross sections is estimated to be about 20% (Table I). The error is primarily due to uncertainties in the background subtraction, the target gas pressure, and the detector efficiency calibration. The relative uncertainties in the cross sections with respect to the variation of the projectile energy are typically 10% due to counting statistics, beam integration, and background subtraction.<sup>6,19</sup>

### III. DISCUSSION OF RESULTS

The summed cross sections  $\sigma_P(K) + \sigma_T(L)$  from Table I are plotted in Fig. 4 versus the impact energy. Up to about 200 keV, the cross sections exhibit a thresholdlike increase. Above this energy the cross sections increase slightly with increasing projectile energies.

Several mechanisms for the vacancy production are possible. Transfer of vacancies from higher-lying MO's or the continuum via direct couplings with the  $4\sigma$  may take place at large internuclear distances ( $\sim 1$  a.u.). It can be shown by rough estimates using the binary encounter approximation that this process of direct excitation can be neglected. Therefore, as in the previously investigated Ar+Ar case<sup>9-11</sup> we assume that electron promotion is the dominant vacancy-production mechanism in the investigated collision systems.

In order to understand the vacancy transfer in this promotion process, adiabatic MO diagrams have been calculated for  $B^+$ ,  $C^+$ , and  $N^+$  on Ar as shown in Fig. 5. The calculations have been performed by Wille<sup>22</sup> using the variable screening model.<sup>23</sup> From these MO diagrams it can qualitatively be inferred which process is the most likely one for the inner-shell vacancy production.

At a certain internuclear distance a strong promotion of the  $2p$  electrons of Ar (for  $B^+$  on Ar the  $1s$  electrons of B) occurs. From Figs. 5(a)–5(c), it is evident that this promotion process guides electrons up via the diabatic  $3d\sigma$  MO (dotted curves in Figs. 5). At various "close-coupling points" the electrons may be transferred into the  $4\sigma$ ,  $5\sigma$ , and  $6\sigma$  MO's. The promoted electrons remain in upper levels when the collision partners depart. In order to make this process possible, it is necessary that vacancies exist in the higher-lying MO's. These vacancies are present because of unfilled or partly filled atomic outer shells in the collision partners, e.g.,  $3s$ ,  $3p$ ,  $2p$  shells of the projectiles or the  $3d$  shell of Ar. In addition, filled MO's may be pre-

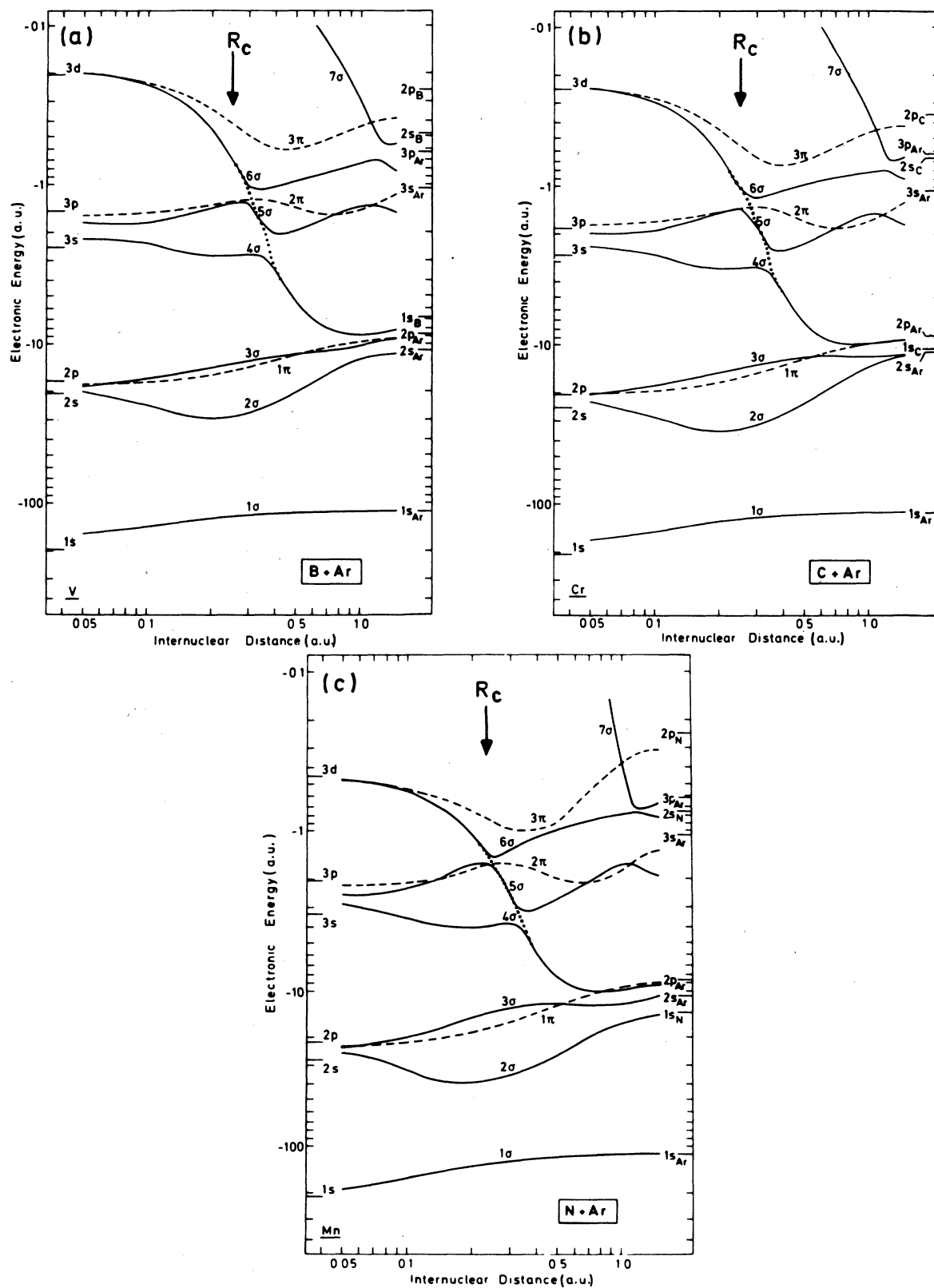


FIG. 5. Adiabatic MO diagrams for the  $B^+$ ,  $C^+$ ,  $N^+$  on Ar collision systems. The diagrams are obtained by applying the variable screening model (Refs. 22 and 23).

emptied by direct ionization processes in the collision.

As the collision proceeds and smaller internuclear distances are reached, an additional transition might occur at smaller internuclear distances (at 0.1 a.u.). Electrons which are guided along the  $3d\sigma$  MO may be transferred via rotational coupling into the  $3\pi$  MO near the united-atom (UA) limit or via the higher-lying empty MO's into the continuum. Hence two possibilities for a vacancy transfer through the  $3d\sigma$  promotion process exist at internuclear distances of roughly 0.1 and 0.2 a.u.

The region where the electrons are lost from the  $3d\sigma$  MO can be roughly estimated from the measured cross sections. Under the assumption that the  $3d\sigma$  electrons are lost in a narrow range near the internuclear distance  $R_c$ , the probability  $P_c$  for  $L$ -shell excitation versus impact parameter follows a step-functional form.<sup>10</sup> Hence, when integrated over impact parameters, the vacancy-production cross section may be expressed as

$$\sigma_L(E) = 2\pi P_c R_c^2 (1 - E_c/E), \quad E \geq E_c.$$

$P_c$  is the probability for electron transitions into empty MO's.  $E_c$  is the impact energy at which the distance of closest approach is equal to  $R_c$  for the zero-impact parameter (see, e.g., Ref. 10). The factor of 2 stems from the fact of two electrons being promoted in the  $3d\sigma$  MO. Cacak *et al.*<sup>10</sup> and Kessel *et al.*<sup>11</sup> have successfully used this model to explain their data from energy loss and Auger-electron measurements for the Ar + Ar system. Moreover, they found that  $P_c$  has to be a value close to 1. In the present analysis it is also assumed that the probability  $P_c$  is close to 1, and the  $R_c$  values are determined from Eq. (1). Very recently measurements of the impact parameter dependence for vacancy production in Ar + C collisions have confirmed that  $P_c$  is close to 1.<sup>24</sup> The values for  $R_c$  are deduced using cross sections at

TABLE II. Estimated "critical internuclear distances" for the  $3d\sigma$  promotion versus projectile  $Z$  as deduced from total cross-section results.

Projectile	Internuclear distances for $3d\sigma$ promotion (a.u.)
B <sup>+</sup>	0.27
C <sup>+</sup>	0.26
N <sup>+</sup>	0.20
O <sup>+</sup>	0.21
Ne <sup>+</sup>	0.14

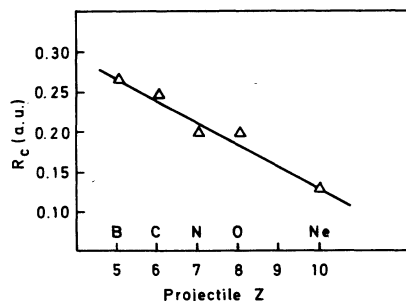


FIG. 6. "Critical internuclear distances" for the  $3d\sigma$  promotion for the different collision systems as obtained from Auger-electron production cross sections (Fig. 4) at 400-keV impact energy.

400-keV impact energy. The results are given as numbers in Table II and they are plotted versus projectile  $Z$  in Fig. 6.

The  $R_c$  values for the transition region are indicated as arrows in Fig. 5. They agree well with the region where the  $3d\sigma$  MO passes through the various close-coupling points in the diagram. In Fig. 6 it can be seen that the  $R_c$  values decrease as the projectile nuclear charge increases indicating that higher- $Z$  projectiles have to interpenetrate the target atom Ar more deeply in order to produce an efficient  $3d\sigma$  promotion. This can be explained by the fact that the  $K$ -shell radius of the projectile ions decreases with increasing  $Z$ .

It should be noted that the energy dependence of the cross sections presented here are somewhat different from earlier reported cross sections for Ar on Ar collisions.<sup>10</sup> There the cross sections showed a steep increase towards projectile energies of about 50 keV while a clear plateau for cross sections above 50-keV impact energies has been formed. Since the cross-section curves in Fig. 4 do not show such a clear plateau, it can be assumed that the step-functional form for the inner-shell excitation probability is not so well fulfilled in the present case. For the case C + Ar it is proven that  $P_c$  is close to one; for the other cases it follows from Eq. (1) that the given  $R_c$  values represent at least lower limits for the transition radii. This shows in particular that vacancy transfer at internuclear distances of about 0.1 a.u. can be excluded.

The described vacancy production process may be a specific feature of the low- $Z$  collision systems which are investigated here. A vacancy transfer at smaller internuclear distances ( $\sim 0.1$  a.u.) as mentioned above is thought to be more likely for heavier collision systems.<sup>13</sup> More insight into the

vacancy-production mechanism should be obtained from a direct measurement of the impact parameter dependence<sup>24</sup> of the excitation probability. The results from those measurements for C + Ar are consistent with the present data.

#### IV. CONCLUSION

Absolute *L*- and *K*-shell vacancy-production cross sections have been deduced from measured Auger-electron-production cross sections for various asymmetric collision systems ( $B^+$ ,  $C^+$ ,  $N^+$ ,  $O^+$ , and  $Ne^+$  on Ar) with projectile energies ranging from 35 to 600 keV. The inner-shell vacancy production for the systems is discussed within the framework of the Fano-Lichten model. The removal of the  $2p$  electron of Ar or the  $1s$  electron of B

proceeds most likely via  $3d\sigma$  electron promotion. Internuclear distances where this promotion takes place have been estimated from the vacancy production cross sections on the basis of a previous model introduced by Kessel and co-workers. The estimated distances coincide with the internuclear distances where the  $3d\sigma$  starts rising rapidly in the calculated adiabatic MO diagrams. It should be noted that we used an indirect method for our analysis from which a certain mechanism for the vacancy production could be favored over others.

#### ACKNOWLEDGMENT

The authors wish to thank Dr. U. Wille for calculating the adiabatic MO diagrams and for helpful discussions.

- 
- <sup>1</sup>U. Fano and W. Lichten, *Phys. Rev. Lett.* **14**, 627 (1965); W. Lichten, *Phys. Rev.* **164**, 131 (1967).
- <sup>2</sup>M. Barat and W. Lichten, *Phys. Rev. A* **6**, 211 (1972).
- <sup>3</sup>K. Taulbjerg, J. S. Briggs, and J. Vaaben, *J. Phys. B* **9**, 1351 (1976); J. S. Briggs, *Rep. Prog. Phys.* **39**, 217 (1976).
- <sup>4</sup>W. E. Meyerhof, *Phys. Rev. Lett.* **31**, 1341 (1973).
- <sup>5</sup>Y. N. Demkov, *Zh. Eksp. Teor. Fiz.* **45**, 195 (1963) [*Sov. Phys.—JETP* **18**, (1963)]; E. E. Nikitin, *Quantum Chemistry*, edited by P. O. Löwdin (Academic, New York, 1970), Vol. 5, p. 135.
- <sup>6</sup>D. Schneider and N. Stolterfoht, *Phys. Rev. A* **19**, 55 (1978).
- <sup>7</sup>E. Bøving, *J. Phys. B* **10**, L63 (1977).
- <sup>8</sup>N. Stolterfoht, *Proceedings of the Invited Lectures at the IX International Summer School on the Physics of Ionized Gases*, edited by R. K. Janev (University Press, Ljubljana, 1979), p. 93.
- <sup>9</sup>B. Fastrup, G. Hermann, and K. J. Smith, *Phys. Rev. A* **3**, 1591 (1971).
- <sup>10</sup>R. K. Cacak, Q. C. Kessel, and M. E. Rudd, *Phys. Rev. A* **2**, 4 (1970); Q. C. Kessel, *Case Studies in Atomic Physics*, edited by E. W. McDaniel, and M. R. C. McDowell (North-Holland, Amsterdam, 1973), Vol. 1, p. 401–462.
- <sup>11</sup>Q. C. Kessel and E. Everhardt, *Phys. Rev.* **146**, 16 (1966).
- <sup>12</sup>R. Fortner, *Phys. Rev.* **185**, 164 (1969).
- <sup>13</sup>W. E. Meyerhof, R. Anholt, and T. K. Saylor, *Phys. Rev. A* **16**, 169 (1977); W. E. Meyerhof, R. Anholt, J. Eichler, and A. Salop, *ibid.* **16**, 190 (1977); W. E. Meyerhof, R. Anholt, J. Eichler, and A. Salop, *ibid.* **17**, 108 (1978); W. E. Meyerhof, *ibid.* **18**, 414 (1978).
- <sup>14</sup>W. N. Lennard and I. V. Mitchell, *Nucl. Instrum. Methods* **132**, 39 (1976).
- <sup>15</sup>N. Stolterfoht, D. Schneider, and D. Brandt, *Abstracts of the Tenth ICAEAC, Paris, 1977*, edited by G. Watel (North-Holland, Amsterdam, 1977), p. 902.
- <sup>16</sup>P. H. Woerlee, R. J. Fortner, S. Doorn, T. P. Hoogkamer, and F. W. Saris, *J. Phys. B* **11**, L425 (1978).
- <sup>17</sup>R. Fortner, *IEEE Transactions on Nuclear Science NS-26, No. 1* p. 1016–1019.
- <sup>18</sup>K. F. Reed, J. D. Garcia, R. J. Fortner, N. Stolterfoht, and D. Schneider, *Phys. Rev. A* **22**, 903 (1980).
- <sup>19</sup>N. Stolterfoht, D. Schneider, D. Burch, B. Aagaard, E. Bøving, and B. Fastrup, *Phys. Rev. A* **12**, 1313 (1975).
- <sup>20</sup>N. Stolterfoht and D. Schneider, see Ref. 17, p. 1130.
- <sup>21</sup>A. Langenberg, F. J. de Heer, and J. v. Eck, *J. Phys. B* **12**, 2079 (1975).
- <sup>22</sup>U. Wille (private communication).
- <sup>23</sup>J. Eichler and U. Wille, *Phys. Rev. Lett.* **33**, 56 (1974); *Phys. Rev. A* **11**, 1973 (1975).
- <sup>24</sup>R. Shanker, R. Bilau, R. Hippler, U. Wille, and H. O. Lutz, 7th International Conference on Atomic Physics, Abstracts of Papers, MIT, Boston, 1980, p. 120.